Expanded View Figures

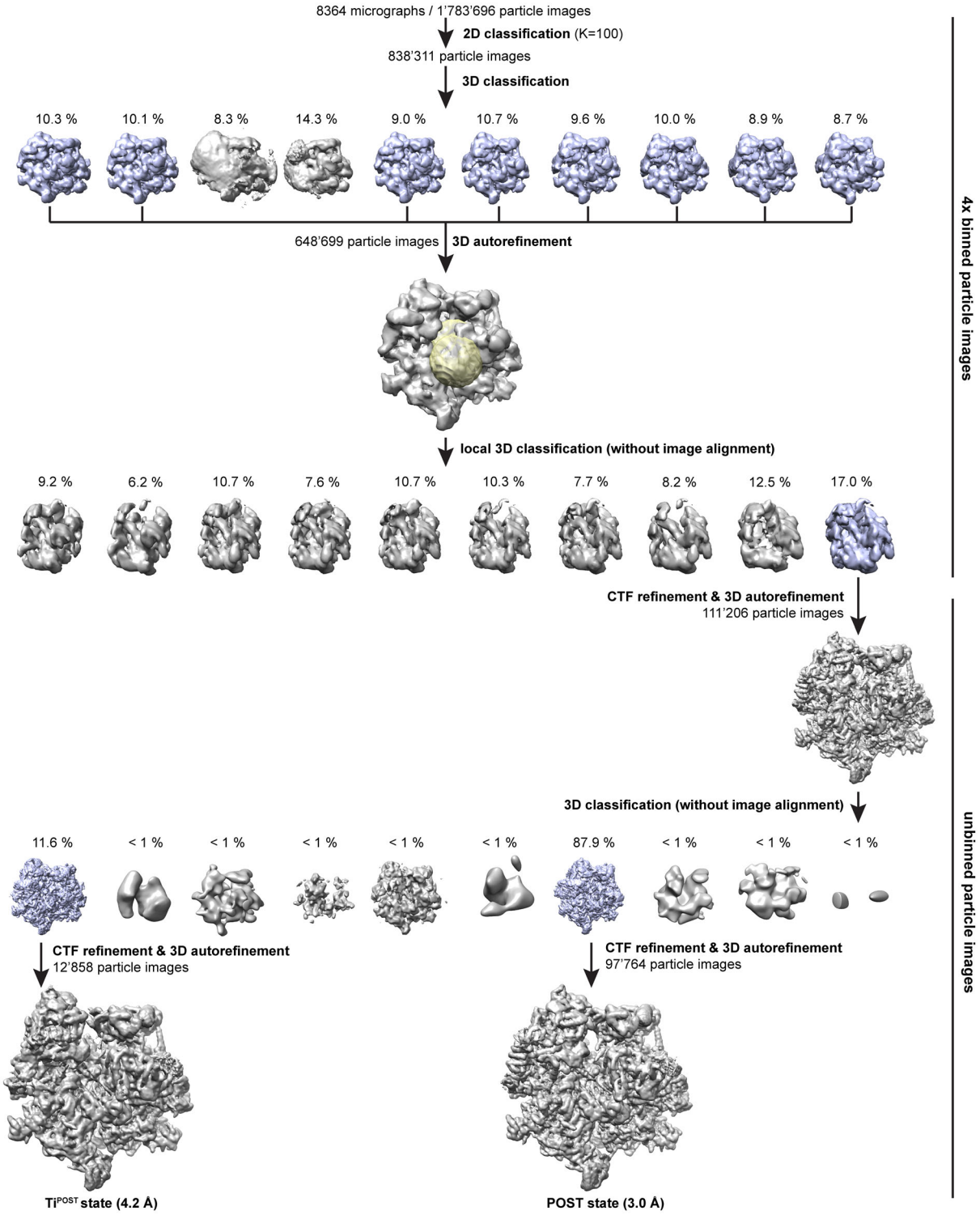

Figure EV1. Particle classification scheme.
During classification, particles were discarded that were either of poor quality or could not be unambiguously interpreted. In each classification step, particles that were retained for further analysis are depicted in violet. The mask used for local 3D classification is shown in yellow superimposed onto the reference.

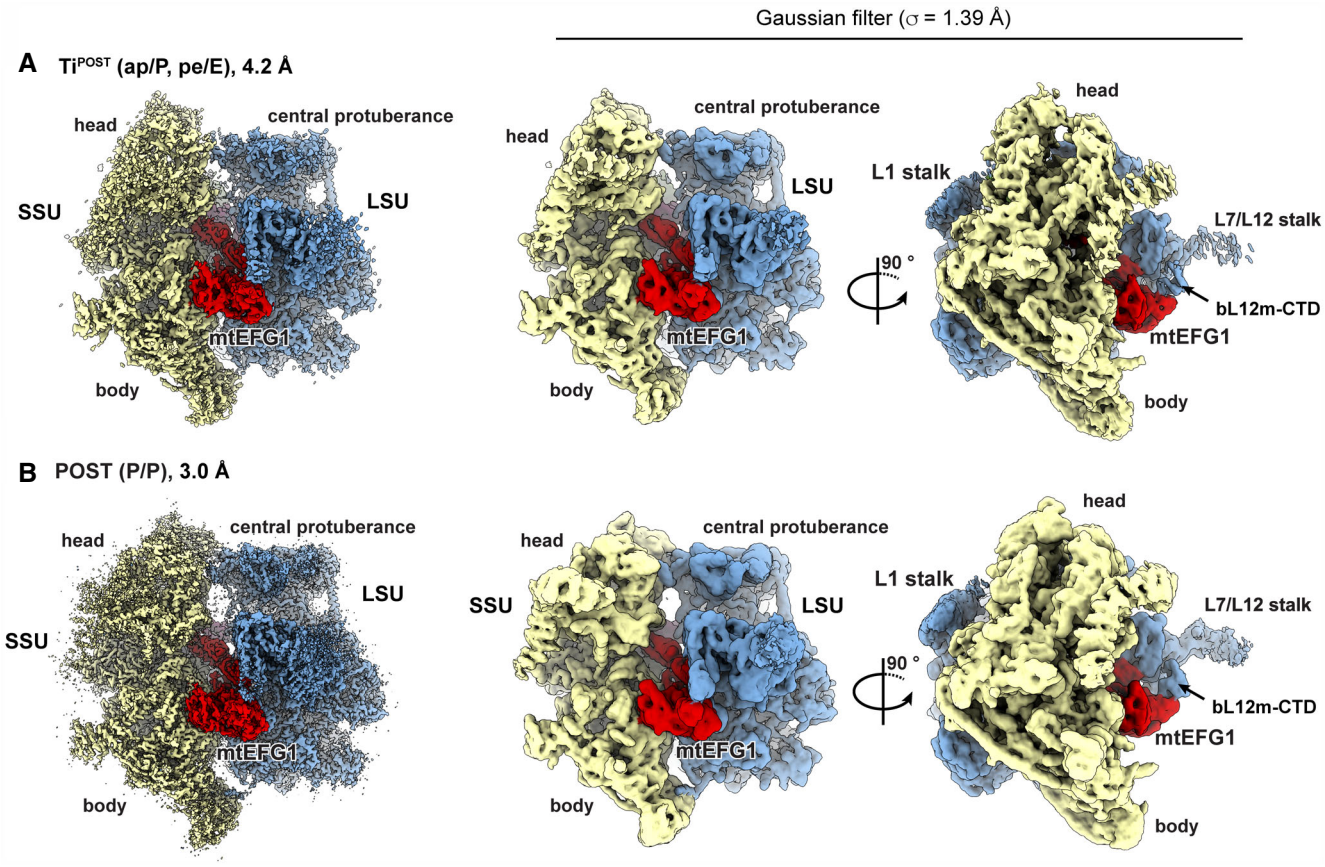

Figure EV2. Experimental EM densities of the Ti^{POST} and POST states.

A Left: The postprocessed EM density of the Ti^{POST} state is shown color-coded according to the underlying structural model (red: mtEFG1, yellow: SSU, blue: LSU). Right: A Gaussian filter (σ = 1.39 Å) has been applied to the EM densities in ChimeraX to visualize also regions of lower resolution. (Goddard *et al*, 2018) EM densities are shown from two different viewing angles.

B The POST state is shown in the same manner as the Ti^{POST} state in (A).

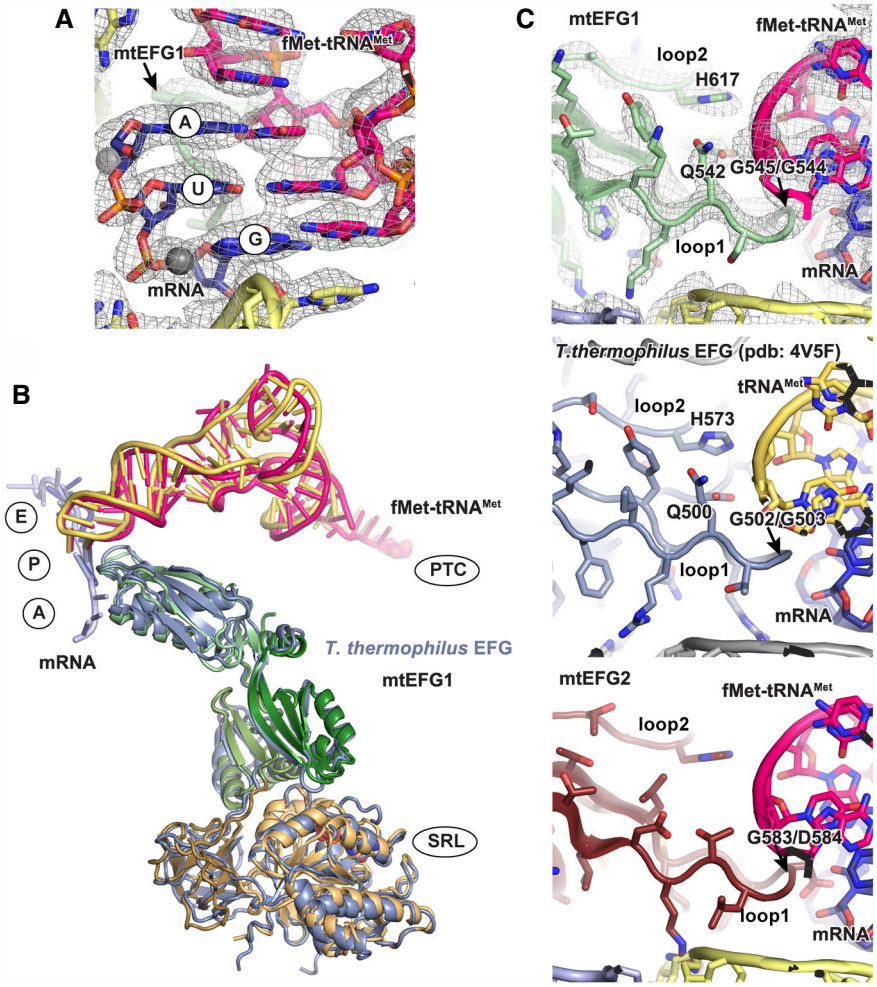

Figure EV3. Interaction of mtEFG1 with the tRNA-mRNA module.

A Codon–anticodon interaction of the tRNA-mRNA module in the POST state. mtEFG1 loop 1 that nestles into the minor groove of the module is shown in light green.

B Superposition of EFG (gray blue), tRNA (yellow), and mRNA (light blue) from the bacterial post-translocation state (PDB: 4V5F) (Gao *et al*, 2009) with the mitochondrial POST state (mtEFG1 color-coded according to Fig 2D, fMet-tRNA^{Met} in pink and mRNA in deep blue). The overall conformation of the bacterial elongation factor and mtEFG1 is very similar as is the interaction of the translation factors with the tRNA-mRNA module. Important ribosomal regions surrounding the elongation factor and the tRNA-mRNA module are indicated (SRL: sarcin–ricin loop, PTC: peptidyl-transferase center on the large mitoribosomal subunit; A,P,E: A, P, E sites on the small mitoribosomal subunit).

C Interactions of different elongation factors with the tRNA-mRNA module. Upper panel: Interaction of mtEFG1 domain IV loops 1 and 2 with the mRNA-tRNA module in the P site of the POST state. Residues conserved in bacteria and important to establish the contact are highlighted. Middle panel: Bacterial EFG in the post-translocation state is shown for comparison (pdb: 4V5F) (Gao *et al*, 2009). Lower panel: A Phyre2 homology model of mtEFG2 (ruby) has been superimposed on mtEFG1 using the POST state of elongation in mitochondria. Neither the critical di-glycine motif nor Q542 that makes stabilizing interactions with the tRNA backbone are conserved.

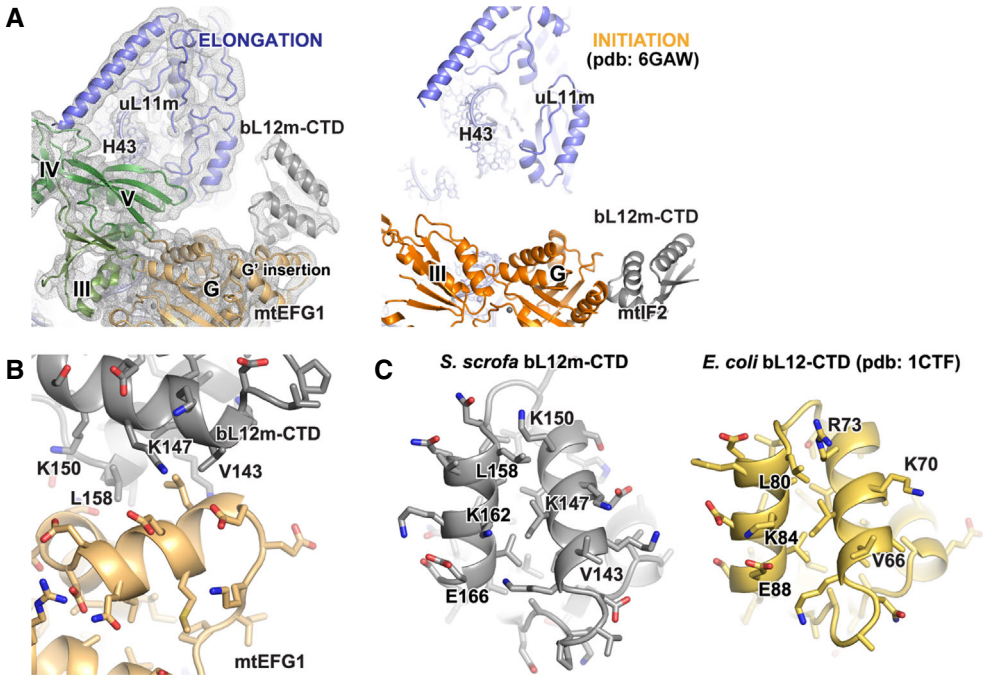

Figure EV4. Overview of the GAC in the mitochondrial elongation and initiation complexes.

A 16S rRNA of the LSU in the initiation and elongation complexes has been superimposed to enable a direct comparison of both complexes using the exactly same view. The different interaction sites of the bL12m-CTD on mtEFG1 (color-coded according to Fig 2D) and mtIF2 (orange) are visible. Moreover, it becomes apparent that mtEFG1 engages in a close interaction with H43 of 16S rRNA as well as uL11m, leading to a downward motion of these elements onto the factor. In contrast, mtIF2 does not contact these elements in the initiation complex.

B A Phyre2 model of the bL12m-CTD has been rigid-body fitted into the EM density of the POST state. The interaction site of the bL12m-CTD (gray) with the G′ insertion of the G domain of mtEFG1 is shown (light orange).

C For comparison, the interfaces of bL12m-CTD (*S. scrofa*, gray) and bL12-CTD (*E. coli*, yellow, pdb: 1CTF Leijonmarck & Liljas, 1987) that contact the mitochondrial or bacterial elongation factor, respectively, are shown. Key residues for interaction with the G domain of translational GTPases are conserved.

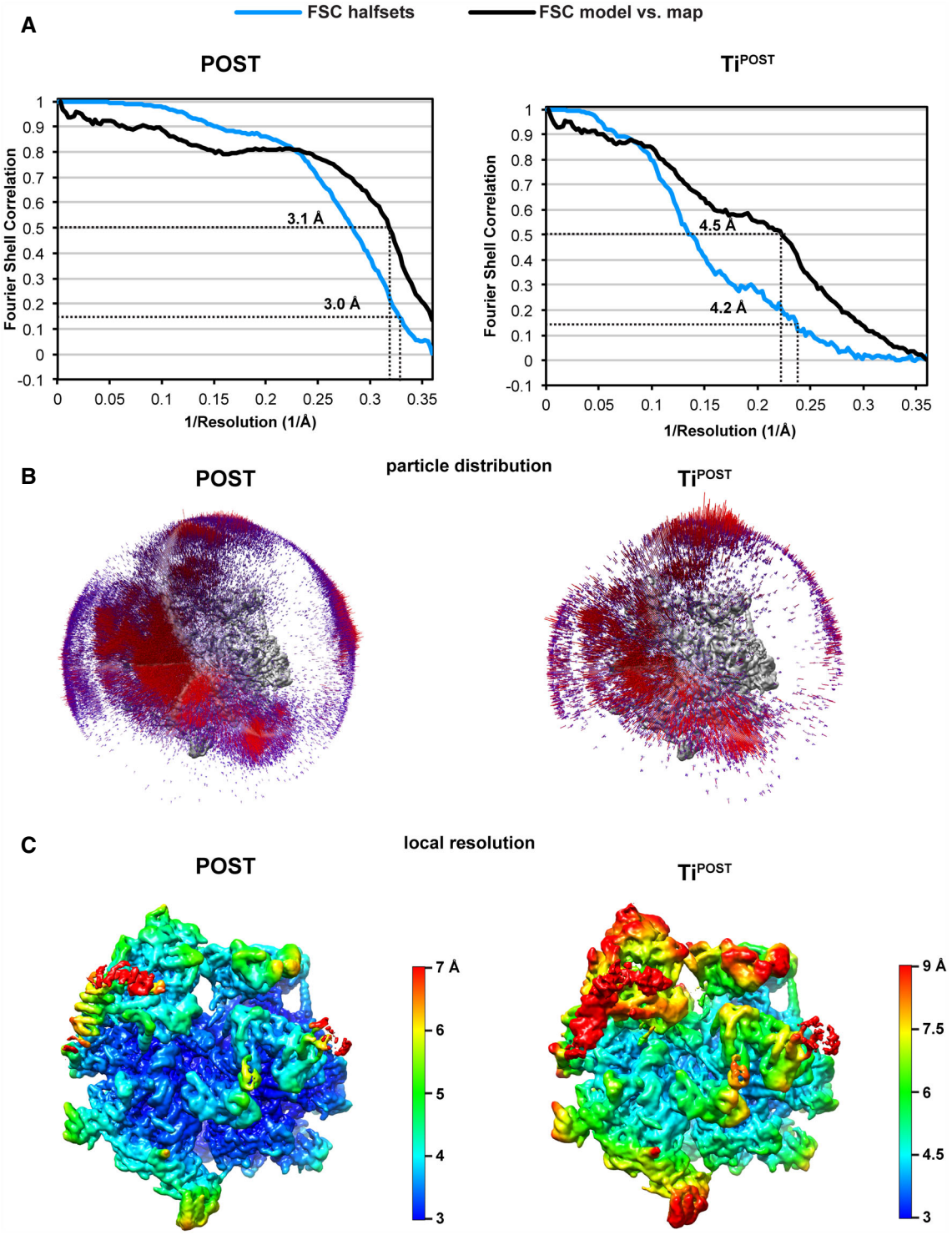

Figure EV5. Map evaluation.

A FSC curves of the halfsets and model versus map for both states are shown with the dashed lines indicating the respective resolution estimates at 0.143 and 0.5 FSC. Curves are plotted until Nyquist (2.78 Å or 0.36 $Å^{-1}$).

B The particle distribution in the final reconstructions is shown superimposed onto the corresponding EM densities.

C Local resolution estimation was done using the implemented algorithm in RELION 3.1 and has been plotted onto unpostprocessed maps for both states (Zivanov *et al*, 2018).